

# Molecular Basis for the Structure and Function of the Xanthine Family of Molybdenum Enzymes

## Estrutura e Função das Enzimas de Molibdénio Pertencentes à Família da Oxidase da Xantina

MARIA JOÃO ROMÃO

INSTITUTO DE TECNOLOGIA QUÍMICA E BIOLÓGICA, APT. 127, 2780 OEIRAS and INSTITUTO SUPERIOR TÉCNICO, DEP. QUÍMICA, 1096 LISBOA CODEX, PORTUGAL

This work is based on the X-ray crystallographic analysis of the aldehyde oxido-reductase from *Desulfovibrio(D.) gigas*, a member of the xanthine oxidase family. Its crystal structure is described and comparisons are made with spectroscopic and kinetic studies from the literature. A main emphasis is put on the recent achievements which have contributed towards the understanding of the structure and function of the xanthine oxidase family of molybde, num enzymes - the hydroxylases. Specific mechanistic implications of the crystal structure of the *D. gigas* enzyme are discussed in relation to the xanthine oxidase family of enzymes.

Este trabalho baseia-se na análise cristalográfica da oxido-reductase do aldeído de *Desulfovibrio(D.) gigas*, uma enzima pertencente à família das oxidases da xantina. Após uma descrição da respectiva estrutura cristalina, são feitas comparações com estudos espectroscópicos e cinéticos da literatura, colocando-se uma ênfase particular nas contribuições mais recentes para a compreensão da estrutura e função das hidroxilases de molibdénio. As implicações mecanísticas específicas da estrutura cristalina são discutidas no contexto das enzimas do tipo da oxidase da xantina.

### Abbreviations

*D.* - *Desulfovibrio*

FAD - flavin adenin dinucleotide

Mop - aldehyde oxido-reductase from *Desulfovibrio gigas*

MPT - mononucleotide form of molybdopterin

MCD - molybdopterin cytosine dinucleotide

MGD - molybdopterin guanine dinucleotide

MAD - molybdopterin adenine dinucleotide

MHD - molybdopterin hypoxanthine dinucleotide

XO - xanthine oxidase

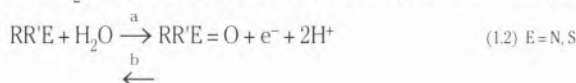
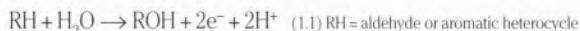
Structural Biology and Chemistry are fields which have greatly benefited and expanded in the years which followed the discovery of X-ray diffraction in 1912 [1]. The application of X-ray Crystallography to the structural analysis of Biological Macromolecules started in the late fifties [2, 3] and ever since is the technique which has more deeply influenced the knowledge of the three-

dimensional structure of proteins, nucleic acids, viruses and other macromolecules: the catalytic centers of enzymes have been unraveled and structure-function relationships established, with important consequences in many domains such as the structure-based *drug design*.

The present article is focused on the crystal structure of a molybdenum enzyme which belongs to the xanthine oxidase family and is the first representative of this group of enzymes for which a 3D structure was determined [7, 8]. Recently, the 3D structures of members of other classes of molybdenum hydroxylases were determined: DMSO reductases [16, 17] and formate dehydrogenase from *E. coli* [69], which however show no homology to the the XO group of enzymes. A description of the basic principles and methodologies used in Protein Crystallography is beyond the scope of this article, but has been outlined elsewhere [4].

## 1. Introduction

Molybdenum containing enzymes can be classified in two classes: 1-nitrogenase, which catalyzes the reduction of dinitrogen to ammonia, and where molybdenum is part of a heterometal FeMo-cofactor [9]; and 2- hydroxylases or oxotransferases, which promote a variety of two-electron oxidation-reduction reactions, whereby oxygen (oxo) atom transfer occurs<sup>1</sup>. Molybdenum plays an essential role in the catalysis of the oxo-transfer reaction, coupled to an electron-transfer between substrate and other cofactors, such as Fe/S centers, hemes or flavins. Coupling of both functions leads to a formal direct transfer of an oxygen atom from the metal center to the substrate. Among the molybdenum hydroxylases which are currently known, xanthine oxidases, sulfite oxidases, nitrate reductases, aldehyde oxidases and DMSO reductases have been characterized in great detail (see [5] for a review). Molybdenum oxotransferase enzymes catalyze the following general reactions, where water has been shown to be the source of the incorporated oxygen atom [10], and reducing equivalents are generated [11, 12].



Xanthine oxidase from bovine milk, due to its ready availability, is the prototype for molybdenum hydroxylases and has been intensively studied for the past forty years, but many other oxomolybdenum enzymes have also been investigated within the last decade. In a recent review on molybdenum oxotransferases [5], these enzymes have been classified into three families on the basis of the reactions they catalyze, as well as on

the basis of the characteristics of their molybdenum centers: (1) The xanthine oxidase family, (2) the sulfite oxidase and assimilatory nitrate reductases family and (3) the DMSO reductase family. This classification is supported by amino acid homologies within these protein families, which are found in a wide range of organisms. The large xanthine oxidase family of enzymes may be considered as the one of the true hydroxylases, with the dithiolene moiety of the molybdopterin cofactor (*fac*) (Figure 1) coordinated to an MoOS (H<sub>2</sub>O) unit. The MoOS coordination was suggested by EXAFS experiments [12-14], but the presence of an additional water ligand was established by crystallography [7, 8]. Members of this family have been found broadly distributed within eukaryotes, prokaryotes and archaea. They catalyze the oxidative hydroxylation of aldehydes and aromatic heterocycles in reactions involving a C-H bond cleavage (reaction 1.1). Sulfite oxidase and assimilatory nitrate reductases possess a *fac*MoO<sub>2</sub> unit, with uncertainty about additional coordination positions of the molybdenum. They have been found in eukaryotes and catalyze a simple oxo transfer to the lone pair of sulfur in sulfite oxidase (E=S, reaction 1.2-a) or the reverse reaction in nitrate reductase (E=N, reaction 1.2-b). In the DMSO reductase family, other enzymes such as the biotin-S-oxide reductase and bacterial dissimilatory nitrate reductases have been included, which also follow the overall stoichiometry of reaction 1.2-b. This family of enzymes possesses the Mo-cofactor with a bisdithiolene coordination of the molybdenum, as recently established by X-ray crystallography [16, 17]. These studies showed that the Mo atom is also coordinated by the side chain oxygen of a serine (Ser 147). This class of enzymes seems to be structurally more diverse when compared to the other two, and its members have only been found in bacteria and archaea.

The molybdenum containing hydroxylases, in particular xanthine oxidases, have been extensively

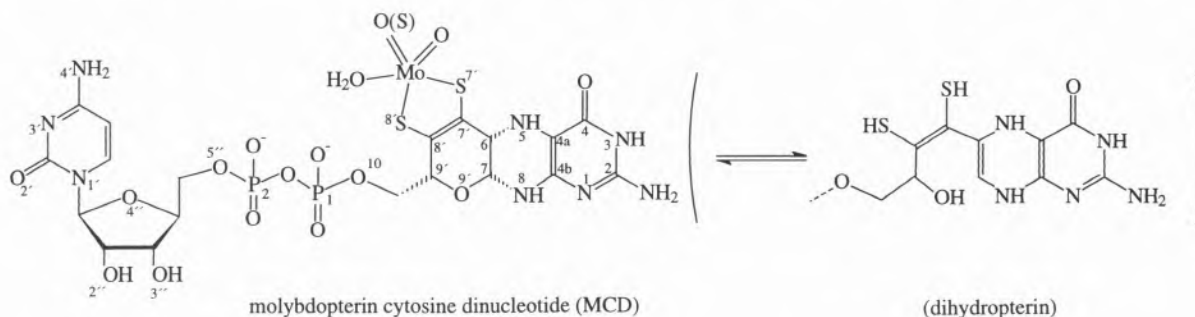


Figure 1 - The molybdenum coordination, with metal ligand distances obtained by EXAFS for Mop [18] and for xanthine oxidase XO [13, 15], in oxidized and reduced forms.

<sup>1</sup> There is complementary as well similarity in the chemistries of molybdenum and tungsten, and pterin-containing tungsten enzymes have also been isolated and characterized, primarily from hyperthermophilic Archaea [27]

studied by a wealth of experimental techniques [5, 6] but a detailed knowledge of these enzymes has suffered from the lack of crystal structures for members of this class. The aldehyde oxido-reductase from *Desulfovibrio (D.) gigas* -Mop- is the first representative of this important group of metalloproteins for which a high-resolution crystal structure is available [7, 8]. In this work we will concentrate on the xanthine oxidase family of molybdenum enzymes with emphasis on the crystal structure of Mop. The functional and mechanistic implications of the Mop structure on a general catalytic mechanism for the xanthine oxidase family of enzymes are an important consequence of this study.

## 2. Brief survey of the xanthine oxidase family of molybdenum enzymes

Molybdenum oxotransferases, in general, possess a common Mo=O group in the metal coordination sphere, reason why they have been called oxomolybdenum enzymes [6]. The molybdenum hydroxylases, which constitute the xanthine oxidase family (containing an MoOS unit) have been assigned on the basis of their irreversible inhibition by cyanide which reacts with Mo=S, releasing thiocyanate. Until X-ray structural data were available for this class of enzymes, the main techniques used to study the molybdenum coordination sphere have been EXAFS [13, 14] (and [18] for Mop) and EPR from the Mo<sup>V</sup> species [19] (and [20, 21] for Mop). EXAFS data have shown that the metal center in its oxidized form has at least one oxo group with a distance Mo=O of about 1.7 Å, as well as two thiolate ligands at distances of about 2.4 Å (see Figure 2). This latter feature is common to all oxomolybdenum enzymes, and is due to the coordination of molybdenum to an organic cofactor commonly designated by "molybdopterin" (Figure 1, left). In spite of the lability of this cofactor when isolated from the protein matrix, its basic pterin ring structure and dithiolene side chain were proposed on the basis of chemical and spectroscopic analysis of the cofactor isolated from the enzymes in different modified or inactivated forms [22-26]. However, the presence of a pyran ring in the structure was established only by crystallography for the tungsten-containing aldehyde oxido-reductase from *Pyrococcus furiosus* [27], for the aldehyde oxido-reductase from *Desulfovibrio gigas* (Mop) [7] and more recently, for the DMSO Reductases from two *Rhodobacter* species [16, 17].

The molybdopterin cofactor is coordinated to the metal via its dithiolene function and may be present either in dinucleotide forms or in the simpler monophosphate form. In Mop, the cofactor is the dinucleotide of cytosine -molybdopterin cytosine dinucleotide (MCD) -, but in other enzymes from prokaryotic sources is found as guanine (MGD) [28], adenine (MAD) [29] or hypoxanthine (MHD) [29] dinucleotide. The simpler monophosphate form (MPT), also found in some bacterial enzymes, is the only form present in all known enzy-

mes from eukaryotic sources and the diversity of the pterin cofactor within known molybdenum-containing enzymes seems to be related to the species of origin rather than the enzymatic function, as shown within the xanthine oxidase family, where MPT has been found in eukaryotic enzymes and MCD in bacterial enzymes reported so far [5].

Members of the xanthine oxidase family show about ~25% sequence identity and 60-70% sequence similarity, with higher conservation in segments involved in the binding of the metal centers and redox-active sites [30]. Enzymes included in this class are either homodimers,  $\alpha_2$ , or dimers of heterotrimers,  $\alpha_2\beta_2\gamma_2$ . Mop, aldehyde oxidases and eukaryotic xanthine oxidases and xanthine dehydrogenases are organized as  $\alpha_2$  homodimers, with all redox-active cofactors confined within a single polypeptide chain. The common folding pattern for this group of enzymes, starts with the two [2Fe-2S] domains, followed by a flavin domain (which is absent in Mop and replaced by an extended segment which connects two domains- Figure 6) and finishes with two large domains responsible for binding the molybdopterin cofactor [30]. Other groups of hydroxylases have been included in the xanthine oxidase family of enzymes, due to analogies in their molybdenum centers and the reactions they catalyze: the CO dehydrogenases, the isoquinoline oxido-reductases and nicotine dehydrogenases, all from bacterial and archaeal sources (see [5] for references). They are organized as  $\alpha_2\beta_2\gamma_2$  structures, where the  $\alpha$  subunit binds the two [2Fe-2S] centers, the  $\beta$  subunit the flavin and the  $\gamma$  subunit the molybdenum cofactor.

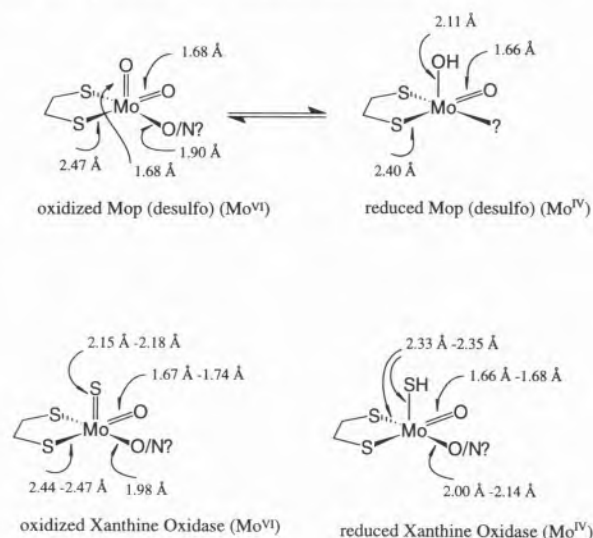


Figure 2 - The molybdopterin cytosine dinucleotide (MCD) cofactor as established by crystallography in Mop [7]. The open chain form is shown as an equilibrium between the two forms (as suggested in solution).



Xanthine oxidase, the prototype of the molybdenum hydroxylases, has been intensively studied by spectroscopic and kinetic techniques, which have contributed to characterize it from a structural and functional point of view. Several inorganic model systems have also been proposed and are described in a number of recent reviews [31-34]. Some attention will now be given to the general features of xanthine oxidase, highlighting relevant points which can be illustrated with details from the crystal structure of Mop.

Xanthine oxidase catalyses the oxidation of xanthine to uric acid, using dioxygen as the physiological electron acceptor (or NAD<sup>+</sup> in the case of xanthine dehydrogenases). In addition to xanthine, it can also oxidize other aromatic heterocycles and aldehydes, but with little specificity. Xanthine is oxidized at the molybdenum center, whereby MoVI is reduced to MoIV and reducing equivalents are transferred to O<sub>2</sub> at the flavin site. Electron transfer between the molybdenum center and the FAD is mediated by the Fe/S centers. Intramolecular electron transfer within the xanthine oxidase family of molybdenum enzymes is an essential aspect of catalysis and has been studied by different techniques such as flash photolysis, pulse radiolysis and pH-jump perturbation (see 5 for references).

EPR was one of the first tools employed for the study of the molybdenum center of xanthine oxidase, and a variety of Mo<sup>V</sup> species were detected, either in the course of equilibrium reductive titrations, or transiently within reaction with substrate. Other characteristic EPR signals have been observed from complexes of the enzyme with inhibitors such as arsenite [35], methanol [36], ethylene glycol [37] and alloxanthine [38], and analogies are encountered between the EPR spectra of XO and those of Mop [20, 21, 39]. For example, the Mo<sup>V</sup> EPR signals ("type 2"), exhibited by xanthine oxidase upon reaction with xanthine [40] ( $g_{1,2,3}$  = 1.9951, 1.9712, 1.9616) are quantitatively very similar to the corresponding signals reported for Mop upon reaction with salicylaldehyde [20] ( $g_{1,2,3}$  = 1.9882(3), 1.9702(3), 1.9643(3)), which suggests similarities of their active sites.

The two [2Fe,2S] centers - Fe/S I and Fe/S II -, are also clearly distinguished on the basis of their characteristic EPR signals, which display similar features in Mop [21] and xanthine oxidases: the so-called Fe/S type I shows characteristic g-values similar within eukaryotic xanthine oxidases (milk XO [36]  $g_{1,2,3}$  = 2.022, 1.935; 1.899) and Mop [21] ( $g_{1,2,3}$  = 2.021, 1.938; 1.919) typical of spinach ferredoxin ( $g_{1,2,3}$  = 2.02(1), 1.93(1), 1.90(1)). On the other hand, center Fe/S II, exhibits broader lines than center Fe/S I, with g-values comparable in Mop [21] (2.057, 1.970, 1.900) and milk xanthine oxidase [68] (2.12, 2.01, 1.91), but displaying larger variations within members of the xanthine oxidase family than the center Fe/S I.

Mössbauer spectroscopy also allows the distinction between both Fe/S centers in the reduced enzymes: one of the centers (probably Fe/S I) exhibits a rather normal

quadrupole splitting  $\Delta E_Q$  of 2.4 mm/s and 2.69(2) mm/s for the ferrous site in xanthine oxidase (at 175K) [41] and Mop (at 180K) [42] respectively, while the other center exhibits an unusually large quadrupole splitting of 3.2 mm/s and 3.14(2) mm/s for xanthine oxidase and Mop respectively.

### 3. The crystal structure of the aldehyde oxido-reductase from *Desulfovibrio gigas*

The crystal structure of Mop, the first representative of a molybdenum oxotransferase, is a valid model for the interpretation of a large number of experimental data of xanthine oxidase and related enzymes. It was solved at high resolution in its native desulfo form [7], as well as in sulfo, oxidized, reduced and alcohol-bound forms [8], allowing a detailed look at the several structural aspects of the molybdenum hydroxylases relevant for catalysis: a) domain architecture; b) structure of the cofactors and binding mode within the polypeptide chain; c) molybdenum center environment; d) metal coordination and its role in catalysis.

In analogy to eukaryotic xanthine oxidases, xanthine dehydrogenases and aldehyde oxidases, Mop is an  $\alpha_2$  homodimer of two 100 kDa subunits (2x907 amino acids) [67]. The redox-active cofactors are two different kinds of [2Fe-2S] centers [21], and a molybdopterin cofactor (molybdopterin cytosine dinucleotide-MCD) (Figure 1), inserted in discrete domains (Figure 3) within a single subunit.

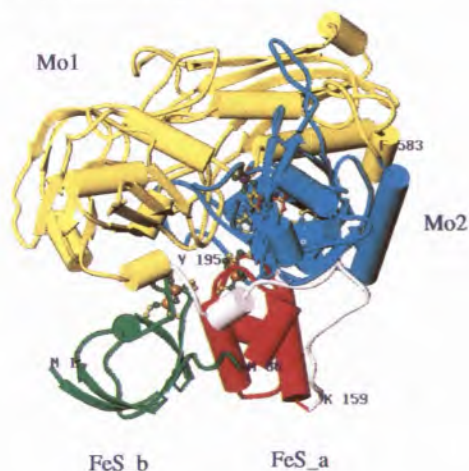


Figure 3 - The molecular structure of Mop with the four independent domains represented in different colors and cofactors shown as colored spheres. Fe/S<sub>b</sub>- green, residues 1-76; Fe/S<sub>a</sub>- red, residues 84-156; connecting peptide-white, residues 158-195; MoI- yellow, residues 196-581; Mo2- blue, residues 582-907.

#### Structural and domain arrangement of the protein

From the electron density map interpretation the two [2Fe-2S] centers were recognized at the earlier



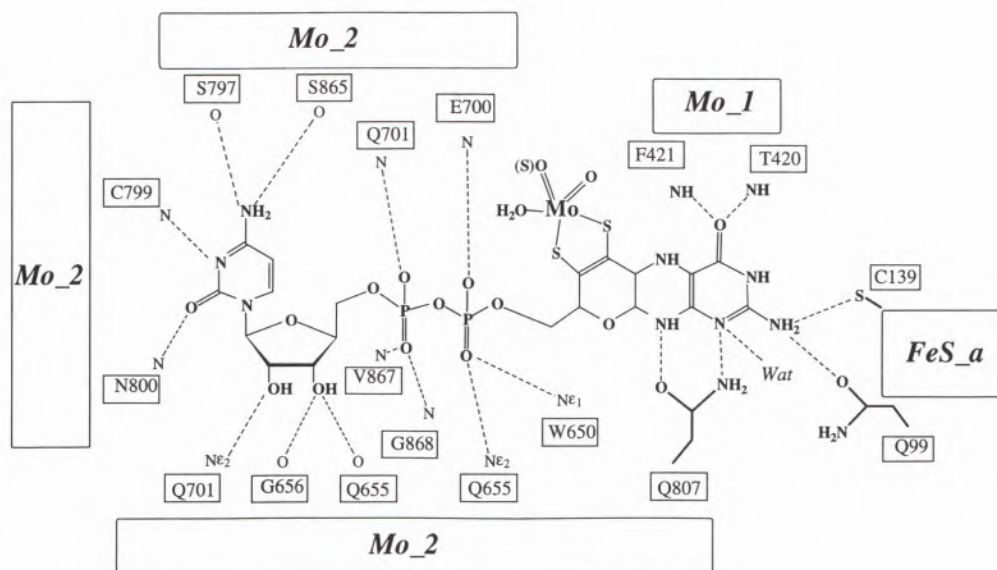


Figure 4 - Stabilization of the molybdopterin cytosine dinucleotide of Mop by hydrogen bonding interactions with surrounding residues (with indication of the domains to which they belong).

stages of the analysis, while the molybdopterin cofactor was identified, only at a later stage of the structure solution, as a molybdopterin cytosine dinucleotide, confirmed by chemical analysis [43]. For some of the higher resolution data sets [8], isopropanol molecules as well as magnesium ions, both from the crystallization solution, were clearly identified. The presence of alcohol molecules, particularly the one close to the molybdenum site (Figure 8), was important for mechanistic deductions, to model the Michaelis complex of an aldehyde substrate molecule (Figure 9).

The protein molecule is roughly globular with an approximate diameter of 75 Å (Figure 3) and its secondary structure shows 28% of  $\alpha$ -helical and 21% of  $\beta$ -sheet conformations. The protein is organized into four domain: two small 2Fe-2S domains (Fe/S\_a and Fe/S\_b) and two much larger domains (Mo1 and Mo2), which constitute the molybdopterin binding portion of the enzyme. The MCD cofactor is bound by a network of hydrogen bonding interactions whereby domain Mo1 contributes with two single molybdopterin binding segments and domain Mo2 binds the other side of the pterin system and provides all of the dinucleotide binding segments (Figure 4). These two large domains also surround the molybdenum catalytic site and define, at their interface, a 15 Å deep tunnel, wide open at the surface and constricted in the middle, which leads substrate molecules into the buried molybdenum catalytic site (Figure 5).

The first Fe/S\_b (residues 1 to 76) domain possesses the consensus sequence **CXXGX $\overline{\text{C}}$ XXC** shared by the plant type ferredoxin class of iron-sulfur proteins [30]. Also the chain fold is similar to that of plant (*Spirulina*

*platensis*) [2Fe-2S] ferredoxins [44]. It shows the topology of a five-stranded  $\beta$ -half barrel with an  $\alpha$ -helix running almost perpendicular to the strands direction. The overall fold can be superimposed to *Spirulina platensis* ferredoxin 44] with a deviation of less than 0.5 Å in the C $\alpha$  atom positions of the iron-sulfur cluster binding turns. The second iron-sulfur domain Fe/S\_a (residues 84 to 156) reveals a unique and new fold for

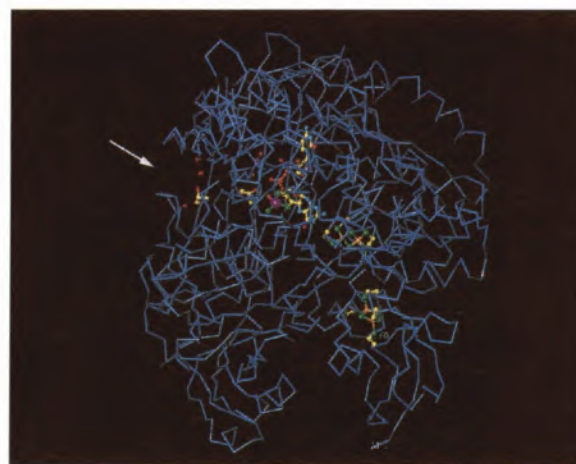


Figure 5 - Simplified C $\alpha$  representation of the Mop molecule with cofactors highlighted as colored spheres. Two isopropanol molecules are also represented as well as the three buried waters close to the molybdenum site (purple sphere). The arrow points towards the entrance of the tunnel, marked also by one of the isopropanol molecules (IPPI) and a few waters.

ferredoxins: a four-helix bundle with two longer central helices flanked by two shorter  $\alpha$ -helices. The metal cluster lies at the N-termini of the two central helices. Domain Fe/S\_a is connected to the molybdenum binding domain Mo1 via a long extended meander with irregular secondary structure and which spans about 50 Å across a rather concave region of the surface of the molecule. This concave region extends from one side of the protein to the other and appears to be the most likely site for the insertion of the flavin domain present in xanthine oxidases. This region of the molecule also appears to be the most probable site of interaction with flavodoxin, which has been shown to be able to accept electrons from Mop/aldehydes *in vitro* [45].

The two larger Moco binding domains, Mo1 (residues 196 to 581) and Mo2 (residues 582 to 907) are in close contact to each other and the molybdenum catalytic site is right at their interface. Domain Mo1 is rather elongated (ca 75 Å long and 28 Å wide) and organized in two subdomains: a larger N-terminal part which consists of a seven-stranded incomplete  $\beta$ -barrel with one  $\alpha$ -helix filling its central cavity with two additional helices flanking the barrel and exposed to solvent. The smaller C-terminal subdomain consists of a five-stranded mixed parallel-antiparallel  $\beta$ -sheet

flanked by two helices which run approximately parallel to the strands direction. Domain Mo2 is also organized in two subdomains, each with a similar basic fold (a four-stranded  $\beta$ -sheet, which bends around a pair of helices), and in part dyad related. Both subdomains resemble two large wings spanning over 80 Å and the co-factor MCD lies at the intersection of those two wings.

### The [2Fe-2S] centers

Both [2Fe-2S] clusters are approximately planar with the two iron atoms and four cysteine sulfur atoms defining a plane orthogonal to the plane of the [2Fe-2S] group. All iron atoms are tetrahedrally coordinated by the sulfur atoms of the cysteines, with Fe-S bond lengths of 2.2 Å and 2.3 Å for the iron-sulfide and for the iron-cysteine  $S^\gamma$  respectively. The N-terminal plant-type ferredoxin iron cluster (Fe/S\_b) has one of the iron atoms linked to C40 and C45, while the other iron atom is coordinated by C48 and C60. The second iron cluster (Fe/S\_a) has one of the iron atoms bound to C100 and C139 and the other bound to C103 and C137. While center Fe/S\_b is close to the protein surface with Cys  $S^\gamma$ 60 exposed to the solvent, center Fe/S\_a is 14 Å buried and in contact with the molybdopterin.

### Xanthine Oxidases

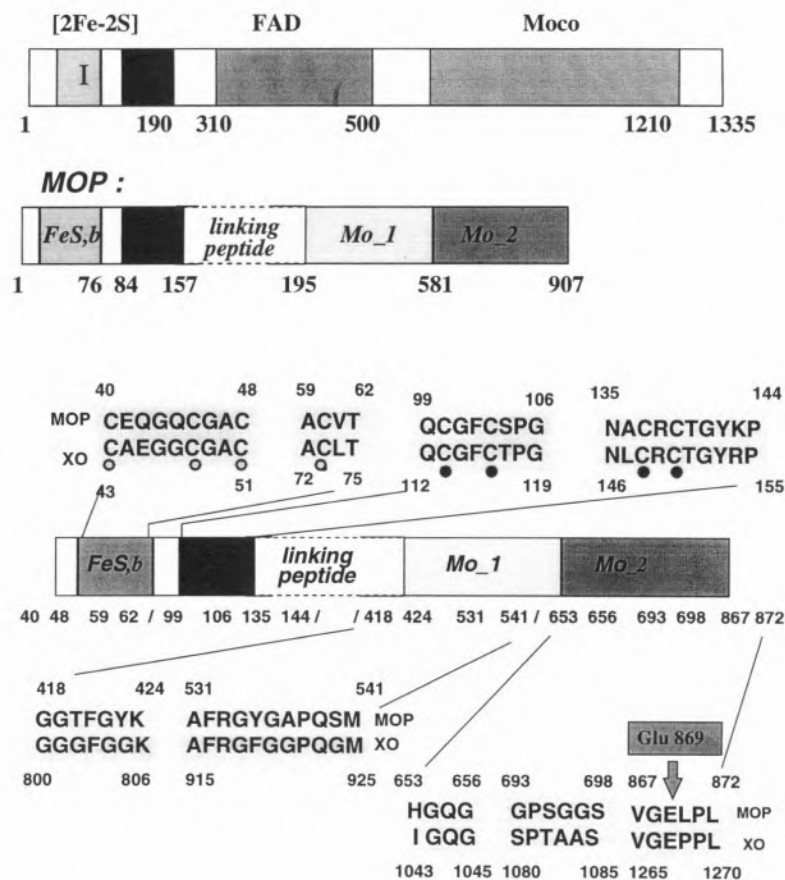


Figure 6 - Primary sequence alignment of Mop and xanthine oxidase. Top-Domain arrangement of xanthine oxidases, in comparison to Mop. Bottom Selection from the amino acid sequence alignment of Mop with xanthine oxidase from *Drosophila Melanogaster* [30], highlighting the conservation of the primary sequence in both proteins, particularly high in the regions involved in co-factor binding.



### The molybdopterin cofactor

The structure of the molybdopterin cofactor was established for Mop by crystallography as a cytosine dinucleotide, MCD (Figure 1). The general bicyclic pterin structure and dithiolene side chain had been proposed by chemical and spectroscopic analysis [22-26], but the fused pyran ring resulting in a tricyclic structure had not been detected and was only established by crystallography. It has now been found in three different enzymes: in the aldehyde ferredoxin oxido-reductase (AOR) from *Pyrococcus furiosus* [27], in Mop [7] and in the DMSO reductase (DMSOR) from *Rhodobacter sphaeroides* [16 and *capsulatus* 17]. In both AOR and DMSOR, the metal atom (W and Mo respectively) coordinates two molybdopterins through their dithiolene groups but in distinct ways. The AOR from *Pyrococcus furiosus* has two molybdopterins coordinating the tungsten atom and additionally linked by a magnesium ion bound to their phosphate groups. In DMSOR two molybdopterin guanine dinucleotides (MGD) are bound to the molybdenum atom resulting in a very elongated structure (~35 Å) [16, 17]. Neither the tungstopterin nor the DMSO reductases share homology to Mop or to the xanthine oxidase family and belong to three different protein families, of which, the DMSO reductase family of oxomolybdenum enzymes is likely to be structurally more diverse than the xanthine oxidase family [5].

When isolated, the cofactor is bicyclic, suggesting that the pyran ring is closed by a reversible intramolecular nucleophilic addition of the hydroxyl 9'-OH to the C7 carbon atom of the double bond of a dihydropterin system (Figure 1). The pyran ring closure may occur *in situ* subsequent to binding of the open chain cofactor to the enzyme favored by the numerous interactions between the cofactor and the surrounding polypeptide chain (cf. Figure 4). In all structures the pyran is tilted approximately 40° relative to the two ring pterin system (<30° in one of the pterins of DMSOR). The fused pyran ring has three chiral centers C6, C7 and C9', with absolute configurations *R, R, R* in Mop, as well as in the other structures. Contrary to suggestions [27, 46] based on functional and structural inorganic models for DMSOR [46], neither the pterin nucleus, nor the dinucleotide coordinate directly to the metal. In DMSOR the protein contributes to the metal coordination with the side chain oxygen of a serine residue, which may be a cysteine or selenocysteine in other members of the DMSOR diverse family.

In Mop the pterin cofactor is in the dinucleotide MCD form and it is well documented [5] that the variants molybdopterin (MPT) and molybdopterin dinucleotides (MGD, MCD, MAD, MHD) are widely distributed among eukaryotes and prokaryotes. In enzymes from eukaryotes the pterin has always been found in the MPT form. The role of the ribonucleotide portion of the molybdopterin dinucleotides in some bacterial enzymes remains obscure.

The MCD present in Mop is extended, with a widest distance of 17 Å between the cytidine (N4' atom) and

the pterin (O4 atom). The functional groups of the cytidine are hydrogen bonded to main chain atoms of domain Mo2 (Figure 4). The structure of this cofactor is likely to represent the general form of dinucleotidic cofactors of other molybdenum hydroxylases, but differences in stabilization of the base are expected, namely in those segments (of domain Mo2) which bind the dinucleotide part, absent in the eukaryotic hydroxylases. This is reflected by the lower degree of homology in this part of the primary sequence, when Mop is compared with eukaryotic xanthine dehydrogenases [30].

### Structure and environment of the metal centers

The redox-active cofactors of Mop are inserted in the protein matrix in close proximity to each other, and define a plausible electron transfer pathway (Figure 7). While the first Fe/S center *b* is rather exposed to solvent via its cysteine 60, Fe/S center *a* is approximately 14 Å below the molecular surface and has no direct contact with the solvent. The closest distance between the iron atoms of the two Fe/S centers is ca. 12 Å while the molybdenum atom lies 15 Å away from the nearest iron atom of center *a*. The molybdenum site is also buried but accessible to the protein surface through a 15 Å deep tunnel as described above. The pterin system of Mo-co is in direct contact with the nearest iron-sulfur center through a hydrogen bond between the amino group at C2 and the  $\gamma$  sulfur atom of Cys139, which coordinates one of the iron atoms. The two iron-sulfur centers are in contact via a chain of seven covalent bonds and a single hydrogen bond between amide of residue Ala136 and the carbonyl of Cys45. The 2Fe-2S iron centers are bound by covalent bonds between the irons and cysteine residues and further stabilized by a number of NH...S hydrogen bonds between their sulfur

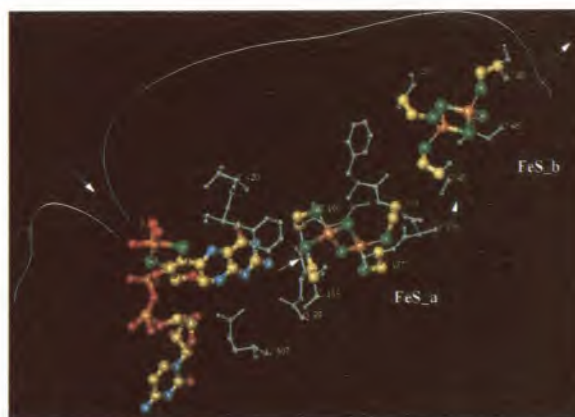


Figure 7 - Molecular representation of the three co-factors of Mop: molybdopterin cytosine dinucleotide and both close contacting centers, FeS<sub>a</sub> and FeS<sub>b</sub>, exposed to solvent through Cys 60. For the sake of clarity, residues contacting with the dinucleotide part are omitted. The arrow shows the direction of the tunnel which leads into the molybdenum site.



After passing the hydrophobic channel reducing substrates, aldehydes in the case of Mop, react and are oxidized at the molybdenum center:  $\text{Mo}^{\text{VI}}$  is reduced to  $\text{Mo}^{\text{IV}}$  and reducing equivalents are transferred through the partially conjugated system of the pterin and the hydrogen bond, pterin-NH2—Sγ-C139, to the Fe/S center a (Figure 7). Electron transfer proceeds via seven covalent bonds and one hydrogen bond (NH Ala136 - - O=C C45) towards the exposed Fe/S center b. From here, electrons will flow to an unknown physiological electron acceptor in the case of Mop or, in the case of xanthine oxidase, will be intramolecularly transferred to the flavin center and from there to molecular oxygen generating superoxide. Intramolecular electron transfer within the xanthine oxidase family of enzymes has been recognized as an essential aspect of catalysis and has been extensively studied by a number of techniques [37-43]. This proposed pathway assigns an important role to the pterin ring for the electron transfer from molybdenum to the Fe/S centers. Since the molybdenum atom is not coordinated to any protein side chain (Figure 8), the pterin cofactor is also essential in anchoring the molybdenum within the protein. A third important role may be attributed to the pterin co-factor by modulating the redox properties of the molybdenum. Crystallographic data of Mop [8] obtained under redu-

Such a role for the pterin cofactor in modulating the redox state of the metal had been proposed [47] on the basis of model compound studies for a Mo<sup>VI</sup> complex L<sub>2</sub>MoO<sub>2</sub> (L=SC(CH<sub>3</sub>)<sub>2</sub>CH<sub>2</sub>NH(CH<sub>3</sub>)), which also exhibits an S – S bond of 2.76 Å, indicative of a disulfide bond character. The authors suggest that the dithiolene group may participate in the Mo<sup>VI</sup> → Mo<sup>IV</sup> redox process by involving a disulfide-thiolate reduction, associated with formal changes of the oxidation state of the metal. Other recent model compound studies [48] have proven that tetrahydropterin is able to reduce MoVI with disulfur coordination (MoO<sub>2</sub>(diethyldithiocarbamate)<sub>2</sub>) to Mo<sup>IV</sup> in (MoO (diethyldithiocarbamate)<sub>2</sub>). These results suggested that oxidation/reduction states of the pterin were involved in the Mo oxidation state during substrate turnover, but extrapolations from these model systems to molybdenum-containing enzymes were not satisfactory. Although the synthesis of such complexes of molybdenum coordinated to pterin species has deserved much attention (reviewed in [32]) and has often been successful [46, 49, 50], the relationship to the reaction mechanism of molybdenum hydroxylases is not clear.

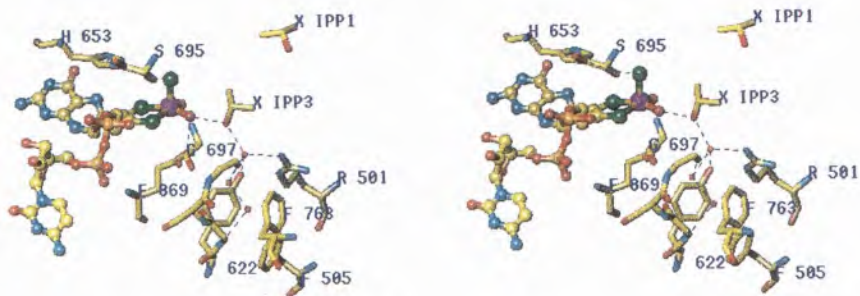


Figure 8 - Stereo representation of the molybdenum catalytic site (sulfo form) and surrounding residues within hydrogen bonding distance. IPP1 points in the direction of the channel and IPP3 is the isopropanol molecule which binds directly to the metal.



There have been proposals in the literature concerning the role of the pterin co-factor in the enzymatic mechanism of the molybdenum oxotransferases. Studies of the state of reduction of MPT in sulfite oxidase [51, 52] and in xanthine oxidase [51] have led to the suggestion of the direct involvement of the pterin in catalysis, either via electron transfer or by modulation of the oxidation/reduction properties of the metal. The Mop crystal structure analyzed in oxidized and reduced states [8] supports these suggestions.

### **The molybdenum site and its environment**

The molybdenum coordination sphere was defined on the basis of the 2.25 Å crystallographic data [7] as square pyramidal geometry, with no protein ligand binding to the metal, but a glutamate residue (Glu 869, conserved within the XO family of enzymes [30] (Figure 6)) is only 3.5 Å away from the metal. With higher resolution data to 1.8 Å [8], the molybdenum site was defined in greater detail and the metal ligands unambiguously identified. In the approximate square pyramidal arrangement, the dithiolene ring system defines the equatorial plane and contributes with two sulfur ligands. The three remaining positions, assigned as three oxygen ligands, were identified as one water ligand (MoOH<sub>2</sub>) and two oxo (Mo=O) groups, where the former occupies the position *trans* to sulfur S7' of the dithiolene (Figure 8). The two oxo groups were identified on the basis of shorter distances to the metal (range of 1.6-1.9 Å for the different crystals analyzed [8]), as well as lack of hydrogen bonds to surrounding residues. The water ligand shows a longer bond to the metal (range of 2.1-2.5 Å) and is within hydrogen bonding contact to the hydroxyl group of isopropanol IPP3, to amide of Gly 697 and to carboxylate of Glu 869 (Figure 8). The apical oxo ligand is found to be replaced by a sulfur atom in Mop crystals which have been resulfurated by incubation with sulfide under turnover conditions [8]. This important result allowed to identify the catalytically essential Mo=S group.

The structure of the molybdenum site agrees with EXAFS data for xanthine oxidases and for Mop, which show an oxo group present in both oxidized and reduced forms of xanthine oxidases and of Mop (Figure 2), while three sulfur ligands are assigned for XO with one longer Mo-S bond for the reduced state of the enzyme. However, EXAFS data did not show the second oxygen ligand, which has now been identified as a coordinated water.

Relevant residues and well ordered water molecules within the molybdenum catalytic site are represented in Figure 8 for the sulfo form of the enzyme. In close vicinity to the molybdenum is the conserved Glu 869 which is approximately *trans* to the apical position and may bind directly to the metal by a small rotation of the carboxylate. The apical Mo=S group has the imidazole of His 653 as nearest neighbor, within hydrogen bonding distance (~3.2 Å). The Mo=O ligand is in a

quite constrained environment, close to amide of Arg 533 (3.3 Å), to carbonyl oxygen of Phe 421 (3.8 Å) and to C $\alpha$  of Gly 422. The metal bound water is facing the mouth of the extended channel and is the most accessible ligand and the neighboring isopropanol molecule (IPP3), from the crystallization solution, contacts with this water ligand. Alcohols are known to inhibit Mop [45] (as well as xanthine oxidase [37]) and this IPP3 site is a good model for the Michaelis complex of the reaction of Mop with aldehydes. The isopropanol molecule is part of a network of hydrogen bonds namely to a chain of three buried water molecules (137W, 138W, 105W). Two of these waters (137W, 138W) are stabilized by hydrogen bonds to the surrounding polypeptide, but the innermost water, 105W, is located in a particularly apolar environment (Phe 505, Phe 763 and Tyr 622) (Figure 8). Apart from IPP3, other isopropanol molecules were located in the crystal structure of Mop, one of which (IPP1) was identified close to the mouth of the channel (Figure 5), which may justify the known inhibitory effect of alcohols in Mop as well as in xanthine oxidase.

To summarize, one can distinguish as most relevant features of this catalytic site: (1) Its accessibility through an extended hydrophobic channel, which has a constriction separating a wider outer compartment from a more restricted inner binding site at the molybdenum; (2) The presence of a water ligand which is the most accessible one, and probably the source of the transferred hydroxyl group and binding site of reaction intermediates; (3) The chain of well ordered buried water molecules, able to replenish the vacant coordination site after product dissociation; (4) The conserved residue Glu 869 close to the molybdenum, which may transiently bind to the metal and act as a proton acceptor of the water molecule (see below).

### **4. Homology of the aldehyde oxido-reductase from *Desulfovibrio gigas* with the xanthine oxidase family of enzymes**

Comparison of the amino acid sequence of Mop with that of different xanthine oxidases was the first proof of their relationship [7, 30]. The multiple alignment with xanthine oxidases from mammalian, insect and fungal sources, showed that the Mop amino acid sequence is highly conserved with ca. 52% homology and 25% identity, suggesting a close structural relationship [30] (Figure 6). Homology also extends to other molybdopterins and iron-sulfur containing enzymes.

The homology is particularly high in those segments associated with binding of the redox-cofactors (but not of the cytosine dinucleotide) as well as within residues of the substrate binding pocket, and for residues of the tunnel. As detailed in Figure 6-b, the binding segments of the cofactors are well conserved. Interruptions by deletions and insertions occur only in

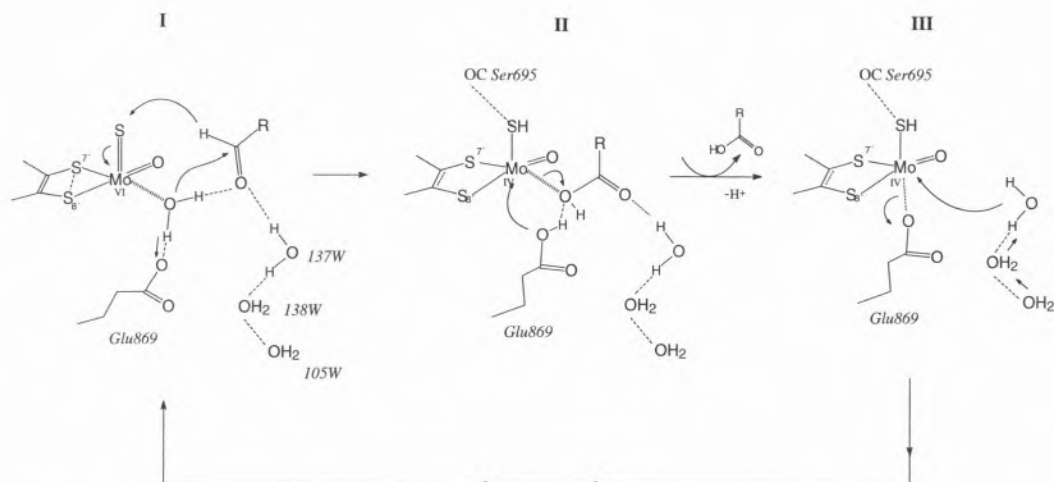


Figure 9 - Hypothetical structures for the reductive half-cycle of the hydroxylation reaction of Mop and xanthine oxidase: I, the Michaelis complex with aldehyde substrate close to MoVI; II, the enzyme/carboxylic acid product complex (MoIV); and III, after product dissociation, intermediate with Glu869

loop regions and at the N- and C- termini. The long deletion of about 400 residues in the Mop structure, between residues 157 and 195, corresponds to the FAD domain in the xanthine oxidases, absent in Mop (Figure 6-a). This additional domain must be placed, in the XO family of enzymes, somewhere along the extended connecting segment (white segment in Figure 3). The FAD binding domain has been tentatively assigned on the basis of mutant studies. A mutation which has received considerable attention is the Tyr395Phe Xanthine dehydrogenase from *Drosophila melanogaster* [53] which was shown to be enzymatically inactive. This residue had been previously shown to be important in the NAD<sup>+</sup> binding by the enzyme, by performing chemical modification of this tyrosine in chicken liver XDH [54]. In all cases, these chemical modifications identified the NAD binding site within the insertion found in the Mop sequence [30].

The close relationship between Mop and the xanthine oxidase family of proteins implies a common mechanism of action of these enzymes and essential structural aspects of Mop agree in fact with a large number of experimental data of the XO class of enzymes.

## 5. Structure based catalytic mechanism

Molybdenum hydroxylases and in particular xanthine oxidases have been investigated by a variety of spectroscopic techniques to gain insight into the mechanism of this class of enzymes. These several aspects have been recently reviewed [5, 6]. In parallel,

much effort has been dedicated to the search for synthetic models of Moco and to the analysis of their structures as well as spectroscopic and functional properties. These model systems and their contribution to the understanding of enzymatic mechanisms have been reviewed [31, 32].

In previous sections we have described relevant features of the Mop structure with important mechanistic implications: (1) The domain organization of the protein and co-factors environment which define a buried catalytic site with unique features; (2) The intramolecular electron transfer among the redox centers, mediated by the pterin cofactor, to which several functions are now clearly associated; (3) The clear definition of the metal coordination sphere, consistent with EXAFS data, as well as the unambiguous location of the catalytically important sulfido molybdenum ligand. The water ligand is revealed for the first time and proposed as the catalytically labile oxygen. The possibility of the water ligand being the source of the labile oxygen is corroborated by recent <sup>17</sup>O-EPR studies [55] of model compounds, on which basis a metal bound hydroxide was proposed as the labile site; (4) The isopropanol site, present in the second coordination sphere of molybdenum is used as a valid model for the Michaelis complex of an aldehyde substrate (Figure 9), whereas the carbonyl oxygen replaces the hydroxyl group and the aldehyde hydrogen occupies the methyl group closer to the metal. In this orientation, the carbonyl oxygen establishes two hydrogen bonds with water 137W and with the water ligand, which polarize it. The nucleophilicity of the water ligand is promoted by Glu 869.



The assumption of the isopropanol site as a model for the substrate binding site is supported by several arguments from the literature: Alcohols are substrate-analog inhibitors of Mop [45] as well as of xanthine oxidase [37], while ethylene glycol is a slow substrate of xanthine oxidase [56]. A number of aldehydes are found to inactivate bovine milk xanthine oxidase [57], while reactivation occurs immediately after removing excess of aldehyde. EPR data of xanthine oxidase inhibited with methanol and formaldehyde produced identical "inhibited" signals [58], suggesting similar binding modes for alcohols and aldehydes. The binding of substrate molecules in the second coordination sphere of molybdenum in the Michaelis complex is also supported by spectroscopic data: In the reaction of xanthine oxidase with 2-hydroxy-6-methylpurine (a slowly reacting substrate), no proton coupling due to the C8-H proton is detected in the "rapid type 1" EPR signal [59], although coupling is detected after substrate oxidation and hydride transfer [59, 60]. Also the strong inhibitor 8-bromoxanthine [61] has been shown to interact with xanthine oxidase in a way typical of purine substrates and the Mo-Br distance was found to be larger than 4 Å.

The structure of the Michaelis complex as represented in Figure 9 shows a simple pathway for the enzymatic reaction: In step I, the carbonyl carbon atom suffers nucleophilic attack by the activated water ligand (transferred as OH<sup>-</sup>), concertedly with hydride transfer to the sulfido group, whereby the carboxylic acid product is generated but remains bound to the molybdenum via the transferred oxygen atom (step II). Bond formation requires a further approach of the atoms involved, possibly via anchoring of the carbonyl oxygen to water 137W, and the aldehyde hydrogen must come closer to the sulfido group. The direct transfer of a hydrogen from substrate (step I) to xanthine oxidase has been detected as a proton from the enzyme strongly coupled to Mo<sup>V</sup> in the rapid EPR signal [62]. The close proximity of the carbonyl carbon atom to the metal as in (II), was proposed in the "inhibited" species of xanthine oxidase, by ENDOR studies [63, 64], while EXAFS has indicated product analogs bound to MoIV [14, 15]. In the last step III, the carboxylic acid product is released, which is probably facilitated by a transient binding of Glu 869 to the metal to maintain a 5-fold coordination. The Mo water site may then be regenerated from the chain of internal buried water molecules.

This reaction scheme agrees with proposals for the reaction of xanthine oxidase [6, 65] and provides details on the exact stereochemical environment. However, it differs by suggesting the water ligand, instead of the oxo group (probably present just as the so-called "spectator oxygen", known from molybdenum coordination chemistry [66], as the labile oxygen to be transferred to the substrate, as supported by recent <sup>17</sup>O-EPR studies 55 and <sup>17</sup>O- and <sup>13</sup>C-ENDOR experiments [63, 64] on xanthine oxidase.

## Acknowledgments

The author thanks the co-authors of papers related to this subject for a most active and productive collaboration, in particular to Prof. José Moura and his group, and to Prof. Robert Huber, whose contribution, dedication and enthusiasm, made this project possible. The support of this work by Project PRAXIS XXI/2/2.1/Bio/05/94 is gratefully acknowledged.

## References

1. W. Friedrich, P. Knipping, M. Laue, *Sitzungsber. Kgl. Bayerische Akad. Wiss.* (1912) 303.
2. J. C. Kendrew, G. Bodo, H. M. Dintzis, R. G. Parrish, H. Wyckoff, *Nature* **181** (1958) 662.
3. R. Huber, P. Reinemer, *Química* **61** (1996) 38.
4. M. J. Romão, *Boletim de Biotecnologia* **53** (1996) 18, and references therein.
5. R. Hille, *Chem Rev* **96** (1996) (in press).
6. R. Hille, *Biochim. Biophys. Acta* **1184** (1994) 143.
7. M. J. Romão, M. Archer, I. Moura, J. J. G. Moura, J. LeGall, R. Engh, M. Schneider, P. Hof, R. Huber, *Science* **167** (1995) 1167.
8. R. Huber, R. Duarte, I. Moura, J. J. G. Moura, J. LeGall, M. Liu, R. Hille, M. J. Romão, *Proc. Natl. Acad. Sci. USA* **93** (1996) 8846.
9. D. C. Rees, J. Kim, M. M. Georgiadis, H. Komiya, A. J. Chirino, D. Woo, J. Schlessman, M. K. Chan, L. Joshua-Tor, G. Santillan, Chakrabarti, Hsu BT, *ACS Symposia* **535** (1993) 170.
10. K. N. Murray, J. G. Watson, S. Chaykin, *J. Biol. Chem.* **241** (1966) 4798.
11. E. I. Stiefel, *ACS Symposia* **535** (1993) 1.
12. R. Hille, *ACS Symposia* **535** (1993) 22.
13. S. P. Cramer, R. Hille, *J. Am. Chem. Soc.* **107** (1985) 8164.
14. R. Hille, G. N. George, M. K. Eidsness, S. P. Cramer *Inorg. Chem.* **28** (1989) 4018.
15. N. A. Turner, R. C. Bray, G. P. Diakun, *Biochem. J.* **260** (1989) 563.
16. H. Schindelin, C. Kisker, J. Hilton, K.V. Rajagopalan, D. C. Rees, *Science* **272** (1996) 1615.
17. F. Schneider, J. Löwe, R. Huber, H. Schindelin, C. Kisker, J. Knäblein, *J. Mol. Biol.* (1996) (in press).
18. S. P. Cramer, J. J. G. Moura, A. V. Xavier, J. LeGall, *J. Inorg. Biochem.* **20** (1984) 275.
19. R. C. Bray, *Quarterly. Rev. Biophysics* **21** (1988) 299.
20. N. Turner, B. A. S. Barata, R. C. Bray, J. Deistung, J. LeGall, J. J. G. Moura, *Biochem. J.* **243** (1987) 755.
21. R. C. Bray, N. A. Turner, J. LeGall, B. A. S. Barata, J. J. G. Moura, *Biochem. J.* **280** (1991) 817.
22. J. L. Johnson, K. V. Rajagopalan, *Proc. Natl. Acad. Sci. USA* **79** (1982) 6856.
23. J. L. Johnson, B. E. Hainline, K. V. Rajagopalan, B. H. Arison, *J. Biol. Chem* **259** (1984) 5414.
24. S. P. Cramer, J. L. Johnson, A. A. Ribeiro, D. S. Millington, K. V. Rajagopalan, *J. Biol. Chem.* **262** (1987) 16357.
25. J. L. Johnson, M. M. Wuebbens, K. V. Rajagopalan, *J. Biol. Chem.* **264** (1989) 13440.
26. K. V. Rajagopalan, J. L. Johnson, *J. Biol. Chem.* **267** (1992) 10199.
27. M. K. Chan, S. Mukund, A. Kletzin, M. W. W. Adams, D. C. Rees, *Science* **267** (1995) 1463.

28. J. L. Johnson, N. R. Bastian, K. V. Rajagopalan, *Proc. Natl. Acad. Sci. USA* **87** (1990) 3190.
29. G. Börner, K. Karrasch, R. K. Thauer, *FEBS Lett.* **290** (1991) 31.
30. U. Thoenes, O. L. Flores, A. Neves, B. Devreese, J. J. V. Beeumen, R. Huber, M. J. Romão, J. LeGall, J. J. G. Moura, C. Rodrigues-Pousada, *Eur. J. Biochem.* **220** (1994) 901.
31. R. H. Holm, *Coord. Chem. Rev.* **100** (1990) 183.
32. J. H. Enemark, C. G. Young, *Adv. Inorg. Chem.* **40** (1993) 1.
33. D. Collison, C. D. Garner, J. A. Joule, *Chem. Soc. Rev.* (1996) 25.
34. R. H. Holm, *Chemistry Rev.* **87** (1987) 1401.
35. M. J. Barber, L. M. Siegel, *Biochemistry* **22** (1983) 618.
36. M. J. Barber, M. P. Coughlan, K. V. Rajagopalan, L. M. Siegel, *Biochemistry* **21** (1982) 3561.
37. D. J. Lowe, M. J. Barber, R. T. Pawlik, R. C. Bray, *Biochem. J.* **155** (1976) 81.
38. T. R. Hawkes, G. N. George, R. C. Bray, *Biochem. J.* **218** (1984) 961.
39. J. J. G. Moura, B. A. S. Barata, *Methods in Enzymology* **243** (1994) 24.
40. S. Gutteridge, S. J. Tanner, R. C. Bray, *Biochem. J.* **175** (1978) 869.
41. F. F. Morpeth, G. N. George, R. C. Bray, *Biochem. J.* **220** (1984) 235.
42. B. A. S. Barata, J. Liang, I. Moura, J. LeGall, J. J. G. Moura, B. Hanh Huynh, *Eur. J. Biochem.* **204** (1992) 773.
43. J. Caldeira, I. Moura, M. J. Romão, R. Huber, J. LeGall, J. J. G. Moura, *J. Inorg. Biochem.* **59** (1995) 739.
44. T. Tsukihara, K. Fukuyama, M. Nakamura, Y. Katsube, N. Tanaka, M. Kakudo, K. Wada, T. Hase, H. Matsubara, *J. Biochem.* **90** (1981) 1763.
45. B. A. S. Barata, J. LeGall, J. J. G. Moura, *Biochemistry* **32** (1993) 11559.
46. B. Fischer, H. Schmalle, E. Dubler, A. Schäfer, M. Viscontini, *Inorg. Chem.* **34** (1995) 5726.
47. E. I. Stiefel, K. F. Miller, A. E. Bruce, J. L. Corbin, J. M. Berg, K. O. Hodgson, *J. Am. Chem. Soc.* **102** (1980) 3624.
48. S. J. N. Burgmayer, A. Baruch, K. Kerr, K. Yoon, *J. Am. Chem. Soc.* **111** (1989) 4982.
49. S. J. N. Burgmayer, M. R. Arkin, L. Bostick, S. Dempster, K. M. Everett, H. L. Layton, K. E. Paul, C. Rogge, A. L. Rheingold, *J. Am. Chem. Soc.* **117** (1995) 5812.
50. S. J. N. Burgmayer, K. Everett, L. Bostick, *ACS Symposia* **535** (1993) 114.
51. S. Gardlik, K. V. Rajagopalan, *J. Biol. Chem.* **265** (1990) 13047.
52. S. Gardlik, K. V. Rajagopalan, *J. Biol. Chem.* **266** (1991) 4889.
53. W. A. Doyle, J. F. Burke, A. Chovnick, F. L. Dutton, C. Russell, J. R. S. Whittle, R. C. Bray, *Biochem. Soc. Trans.* **24** (1996) 31S.
54. T. Nishino, T. Nishino, *J. Biol. Chem.* **264** (1989) 5468.
55. R. J. Greenwood, G. L. Wilson, J. R. Pilbrow, A. G. Wedd, *J. Am. Chem. Soc.* **115** (1993) 5385.
56. S. J. Tanner, R. C. Bray, *Biochem. Soc. Trans.* **6** (1978) 1331.
57. F. F. Morpeth, R. C. Bray, *Biochemistry* **23** (1984) 1332.
58. F. M. Pick, M. A. McGartoll, R. C. Bray, *Eur. J. Biochem.* **18** (1971) 65.
59. R. Hille, J. H. Kim, C. Hemann, *Biochemistry* **32** (1993) 3973.
60. S. Gutteridge, S. J. Tanner, R. C. Bray, *Biochem. J.* **175** (1978) 887.
61. R. Hille, R. C. Stewart, *J. Biol. Chem.* **259** (1984) 1570.
62. R. C. Bray, G. N. George, *Biochem. Soc. Trans.* **13** (1985) 560.
63. B. D. Howes, R. C. Bray, R. L. Richards, N. A. Turner, B. Bennett, D. J. Lowe, *Biochemistry* **35** (1996) 1432.
64. D. Howes, B. Bennett, R. C. Bray, R. L. Richards, D. J. Lowe, *J. Am. Chem. Soc.* **116** (1994) 11624.
65. H. Kim, M. G. Ryan, H. Knaut, R. Hille, *J. Biol. Chem.* **271** (1996) 6771.
66. K. Rappé, W. A. III Goddard, *J. Am. Chem. Soc.* **104** (1982) 3287.
67. M. J. Romão, B. A. S. Barata, K. Lobeck, I. Moura, M. A. Carrondo, J. LeGall, F. Lottspeich, R. Huber, J. J. G. Moura, *Eur. J. Biochem.* **215** (1993) 729.
68. D. J. Lowe, R. M. Lynden-Bell, R. C. Bray, *Biochem. J.* **130** (1972) 239.
69. (a) V. N. Gladyshev, J. C. Boyington, S. V. Khangulov, D. A. Grahame, T. C. Stadtman, P. D. Sun *J. Biol. Chem.* **271** (1996) 8095. (b) J. C. Boyington, V. N. Gladyshev, T. C. Stadtman, P. D. Sun IUCr XVII Congress of the International Union of Crystallography (1996).